COMBINING STRUCTURAL OPTIMIZATION AND STRUCTURAL CONTROL

by
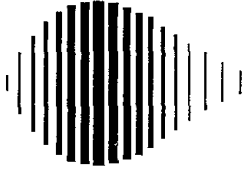
F. Y. Cheng and C. P. Pantelides

Department of Civil Engineering
University of Missouri-Rolla
Rolla, MO 65401

Technical Report NCEER-88-0006

January 10, 1988

COMBINING STRUCTURAL OPTIMIZATION
AND STRUCTURAL CONTROL

by

F.Y. Cheng[1] and C.P. Pantelides[2]

January 10, 1988

Technical Report NCEER-88-0006

1 Curators' Professor, Dept. of Civil Engineering, University of Missouri-Rolla
2 Assistant Professor, Dept. of Civil Engineering, University of Missouri-Rolla

NATIONAL CENTER FOR EARTHQUAKE ENGINEERING RESEARCH
State University of New York at Buffalo
Red Jacket Quadrangle, Buffalo, NY 14261

ABSTRACT

The optimal design of structures subjected to seismic excitations and equipped with active control systems including active tendons, active mass damper and a combination of the two is presented. Optimal and non-optimal control algorithms are employed for implementation of the structural control. The structural optimization is formulated in terms of construction materials or structural weight with various constraints of displacements and control forces. A control energy performance index is also minimized to find optimal weighting matrices that yield the least optimal control forces satisfying the constraints.

A critical-mode control algorithm is derived based on the instantaneous closed-loop technique. The spillover effect is studied theoretically and numerically. The algorithm is then used to establish optimal locations for a limited number of active tendon controllers. Three approaches of using the modal shapes, the performance index of control energy, and the performance index of response are studied for determining the optimal locations.

TABLE OF CONTENTS

LIST OF ILLUSTRATIONS

LIST OF TABLES

SECTION 1

INTRODUCTION

Because of recent advances in electronics, engineers and scientists are on the threshold of a new era in structural analysis and design. Most of their research efforts are based on the development of sophisticated computer programs for the analysis of complex structures. Currently, when these programs are used to design structures, the relative stiffnesses of a structure's constituent members must be assumed. If the preliminary stiffnesses are misjudged, repeated analyses, regardless of a program's sophistication, will usually not yield an improved design. The programs that are presently used are actually based on coventional designs, and their application in reality is an art rather than a science.

The optimum design concept has been recognized as being more rational and reliable than those that require the conventional trial and error process [refs. 3, 26, 31]. It is because for a given set of constraints, such as allowable stresses, displacements, drifts, frequencies, upper and lower bounds of member sizes, and given seismic loads, such as equivalent forces in the code provisions, spectra, or time-histories, the stiffnesses of members are automatically selected through the mathematical logic (structural synthesis) written in the computer program. Consequently, the strengths of the constitutent members are uniformly distributed, and the rigidity of every component can uniquely satisfy the demands of the external loads and the code requirements, such as displacements and drifts. By using an optimum design computer program, one can conduct a project schedule at a high speed and thus increase the benefit because of the time that is saved. An optimum design program can also be used for parametric studies to identify which structural system is more economical and serviceable than the other and assess the principles of various building code provisions as to whether they are as logical as they are intended to be [refs. 4, 10, 16].

Structural control implies that performance and serviceability of a structure are controlled so that they remain within prescribed limits during the application of environmental loads. Structural control is achieved by

SECTION 2

STRUCTURAL OPTIMIZATION

USING NON-OPTIMAL CONTROL

2.1 Structural System

The structural model chosen for the present study is an N-story shear
building equipped with a number of active tendons (AT), and an active mass
damper (AMD), as shown in Figure 2-1. The assumptions made to simplify the
analysis are: 1) the mass of each floor is concentrated at the floor level,
2) linear elasticity is provided by massless columns between neighboring
floors, 3) the structural response is described by the displacement and
lateral force in each story, 4) AT controllers are installed between two
neighboring floors either above or below the jth floor, 5) an AT controller
is regulated by two sensors placed on the floors above and below it, 6) an
AMD is placed on the top floor, and 7) an acceleration sensor is placed at
the top floor to regulate the AMD controller.

2.2 Formulation of Non-Optimal Closed-Loop Algorithm

The procedure for analysis follows the transfer matrix approach in the
frequency-domain instead of the classical modal approach. The transfer
matrix approach determines the structural response directly without having
to calculate the natural frequencies and modes. This results in
considerable simplification of the calculations. The transfer matrix
approach was early studied by Yang [ref. 32]. Two features are different in
the derivations presented herein. First, each floor of the structure does
not have to be identical to the others. This is required for the structural
optimization algorithm to be implemented. Secondly, the present derivation
includes a combined active tendon-mass damper system. It will be shown in
the numerical examples that the combined system resulted in improved
performance of the control system.

The earthquake ground acceleration is modelled as a stochastic process and a
random vibration analysis is carried out to determine the stochastic
response. It is assumed that the statistics are time-invariant, or

$g_m(\omega)$ = AMD controller gain

$k_{cj} = k_j + g_t(\omega)$

$g_t(\omega)$ = AT controller gain

The controller gains $g_m(\omega)$ and $g_t(\omega)$ are functions of thenormalized feedback and loop gains for the AT τ_t and ε_t, and for the AMD τ_d and ε_d, respectively. Note that Eq. (2) is valid for floors 1 to (N-1), and it can be written recursively to transfer the response of the mth floor to that of the (m-1)th floor. Applying the boundary conditions at the top floor and base of the building one can solve Eqs. (2-4) to determine the displacement response $\overline{X}_j$, the shear force $\overline{Y}_j$, and the AMD and AT control forces. Detailed derivation and solution of Eqs. 2-4 are available in [refs. 5, 6].

The structural response and active control statistics are stationary random processes with zero mean. The power spectral density of the jth floor displacement response is given by

$$S_{Xj}(\omega) = \left\| \overline{X}_j \right\|^2 \omega^{-4} \Phi \ddot{X}_g(\omega) \qquad (5)$$

where:

$$\left\| \overline{X}_j \right\|^2 = \text{magnitude of the displacement response}$$

The mean square response at the jth floor, σ^2_{xj}, is

$$\sigma^2_{xj} = \int_{-\infty}^{\infty} \left\| \overline{X}_j \right\|^2 \omega^{-4} \Phi \ddot{X}_g(\omega) d\omega \qquad (6)$$

Similar relations can be written for the shear forces, AT control forces, and the AMD control force.

2.3 Optimization for Non-Optimal Algorithm

From previous studies by Cheng and his associates for deterministic and nondeterministic structural systems [refs. 4, 6, 11, 14, 16], it is known

The quantity σ_{xj} can be obtained from the response statistics of Eq. (6). The quantities σ_{ti}, and σ_d can be obtained from similar equations. The implementation of standard deviation expressed in the constraints is in the sense that for a given maximum displacement and a probability of not exceeding that value, the standard deviation of the displacement can be obtained. A Gaussian probability distribution is assumed. The numerical procedure for the solution of the optimization problem of Eqs. (7) through (13), follows a penalty function formulation.

2.4 Numerical Examples

2.4.1 Example 1: Two-Story Building

The optimization procedure is applied to a two-story building shown in Figure 2-2 for earthquake excitation. The objective is to find the minimum structural weight that satisfies the imposed constraints. The design variables are the floor stiffnesses, and the normalized loop and feedback gains. Three case studies are made. In Case A, the structure is equipped with two active tendons whose stiffness k_t is allowed to vary according to the variation of the jth floor stiffness, k_j, in the optimization procedure as $k_t = 0.05 \ k_j$. In Case B, the stiffness of the tendons is fixed at k_t = 40 kips/in (7000 kN/m). In Case C, an active mass damper is included in addition to the two tendons. The earthquake excitation used is that of Eq. (1), of the Kanai-Tajimi spectral density function, with the following parameters: ω_g = 18.85 rad/sec, ζ_g = 0.65, and S^2 = $4.65 \times 10^{-4} m^2/sec^3/rad$. The structural properties for all three cases are: $m_1 = m_2$ = 2 kip-sec²/in (350 Mg), $c_1 = c_2$ = 1.6 kip-sec/in (280 Mg/sec), and θ = 25 degrees, where θ = angle between the tendon and the grider. The active mass damper parameters for Case C are: m_d = 0.04 kip-sec²/in (7 Mg), k_d = 6.11 kip/in (1070 kN/m), c_d = 0.10 kip-sec/in (17.5 Mg/sec), and k_{md} = 25 kip/in (4378 kN/m), where k_{md} = proportionality constant for active mass damper. The constraints for all three cases are: σ_{x1} max = 0.035 in (0.89 mm), σ_{x2} max = 0.070 in (1.78 mm), σ_{t1} max = σ_{t2} max = 10 kips (44.48 kN), τ max = ε max = 10. Additional constraints are imposed for Case C as $\tau_d \le 6$, and $\varepsilon_d \le 6$.

weight. Comparing the three control configurations, we note from Figures 2-10 and 2-11 that the combined system of Case 4, gives the least weight. The optimum stiffness distribution for all four cases is shown in Figure 2-12. The values of the normalized loop and feedback gains for Case 4 are given in Figure 2-13. It is observed that τ_{t1} reaches upper bound, τ_{t2} is close to the upper bound, but τ_d is low. Similar results are obtained for ε_{t1}, ε_{t2}, and ε_d. The power spectral densities of the response for the four optimal cases were calculated; the spectral density of the eighth floor relative displacement and the spectral density of the base shear force are shown in Figures 2-14 and 2-15, respectively. From these figures it is obvious that the no-control case is the worst case. Cases 3 and 4 control the response effectively; Case 4, however has the least weight and it reduces the higher modes better than Case 3. Case 2 reduces the higher modes best, but of the three control cases has the most weight.
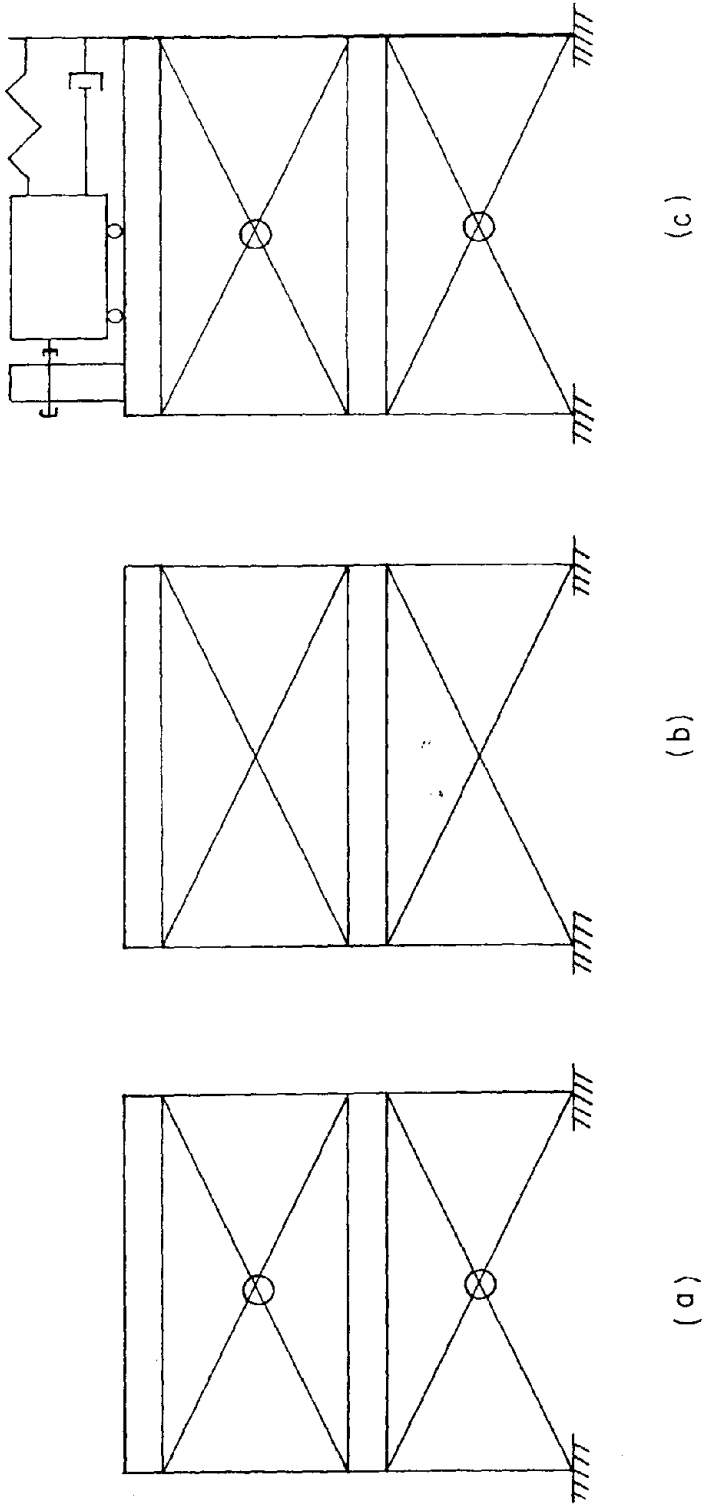
FIGURE 2-2 Two-story Shear Building:
(a) Case A, (b) Case B, (c) Case C
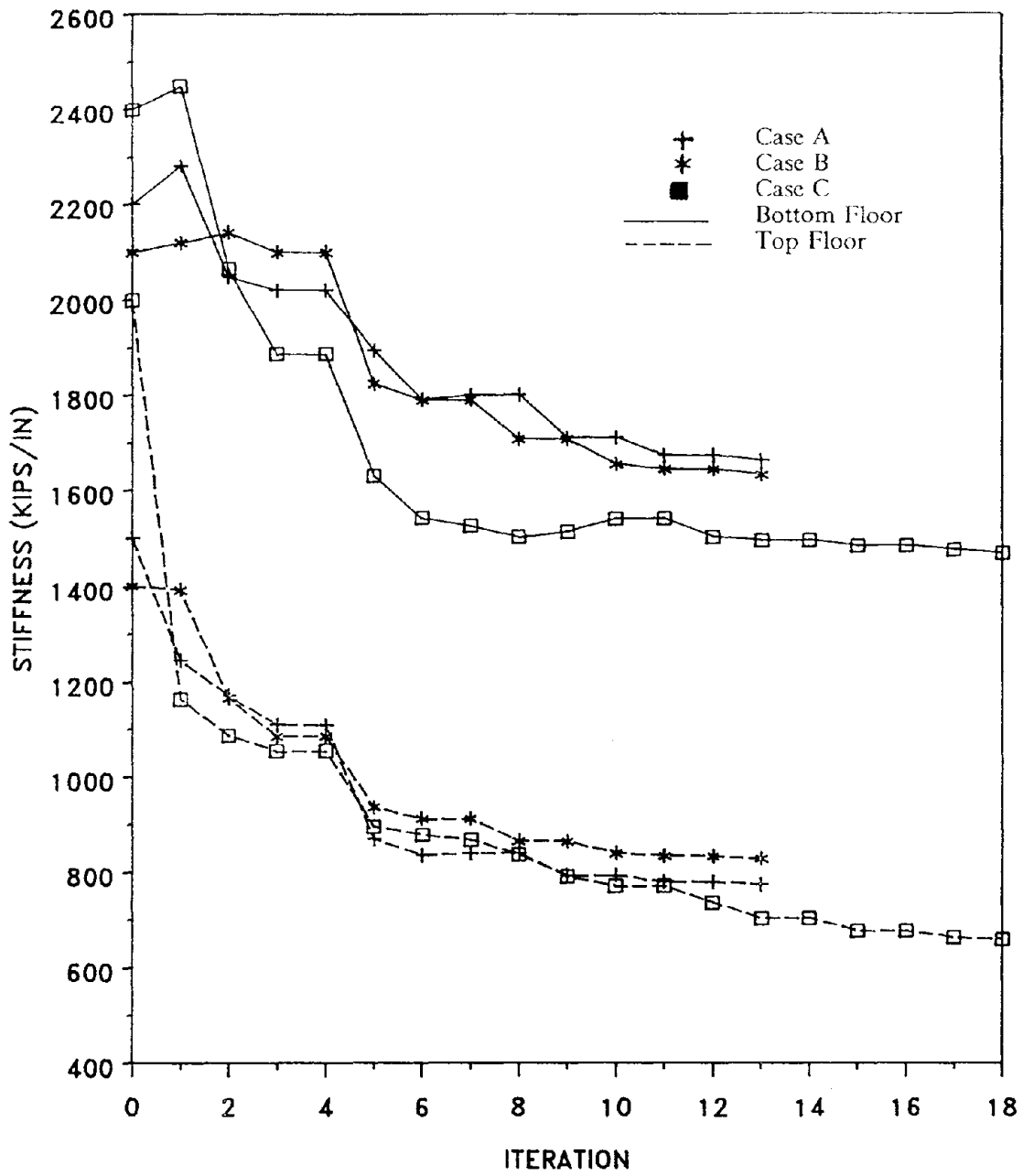
FIGURE 2-4   Structural Stiffness for Cases A, B, and C
(1 kip/in = 175.1 kN/m)
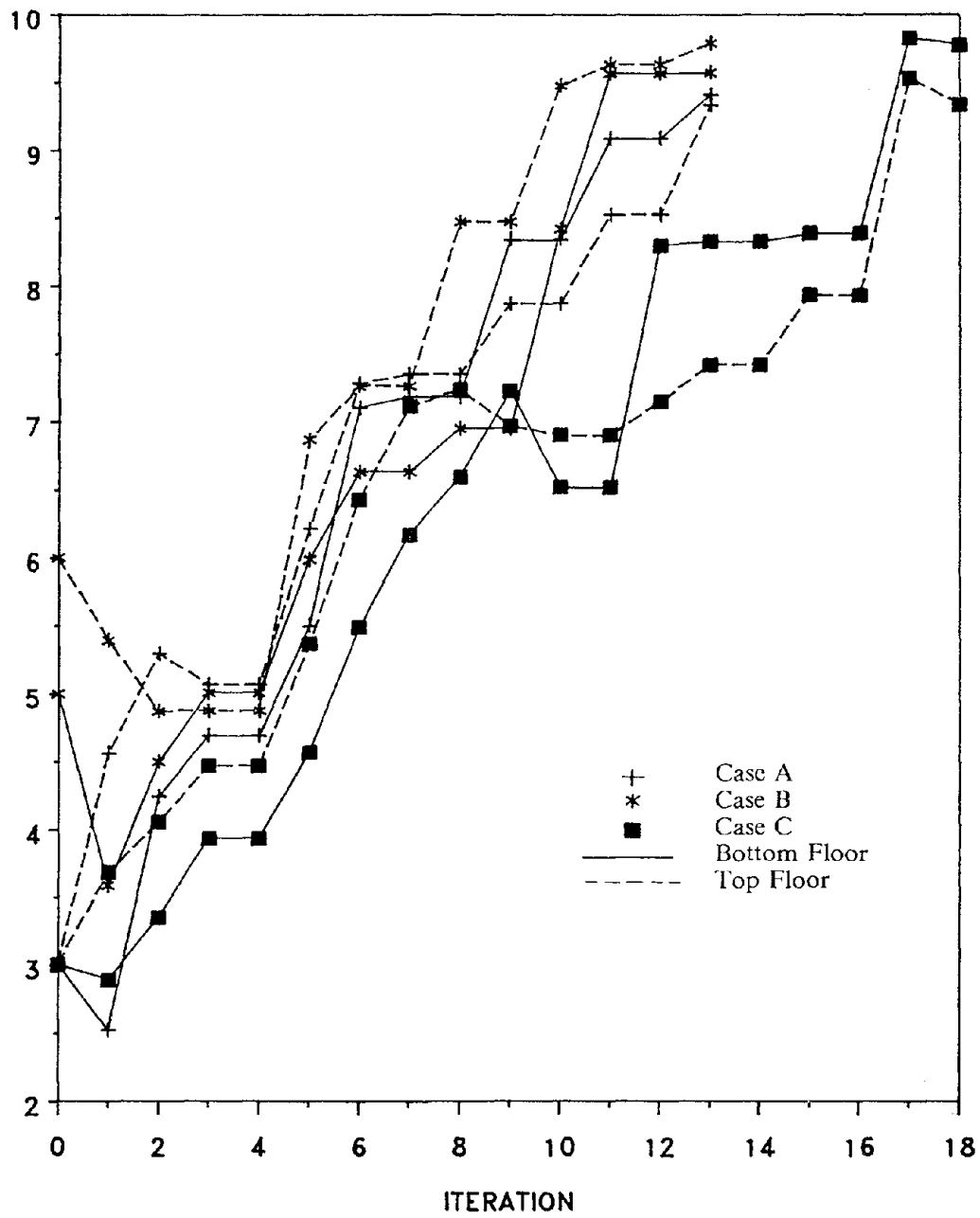
FIGURE 2-6   Normalized Loop Gain of Active Tendons
             for Cases A, B, and C
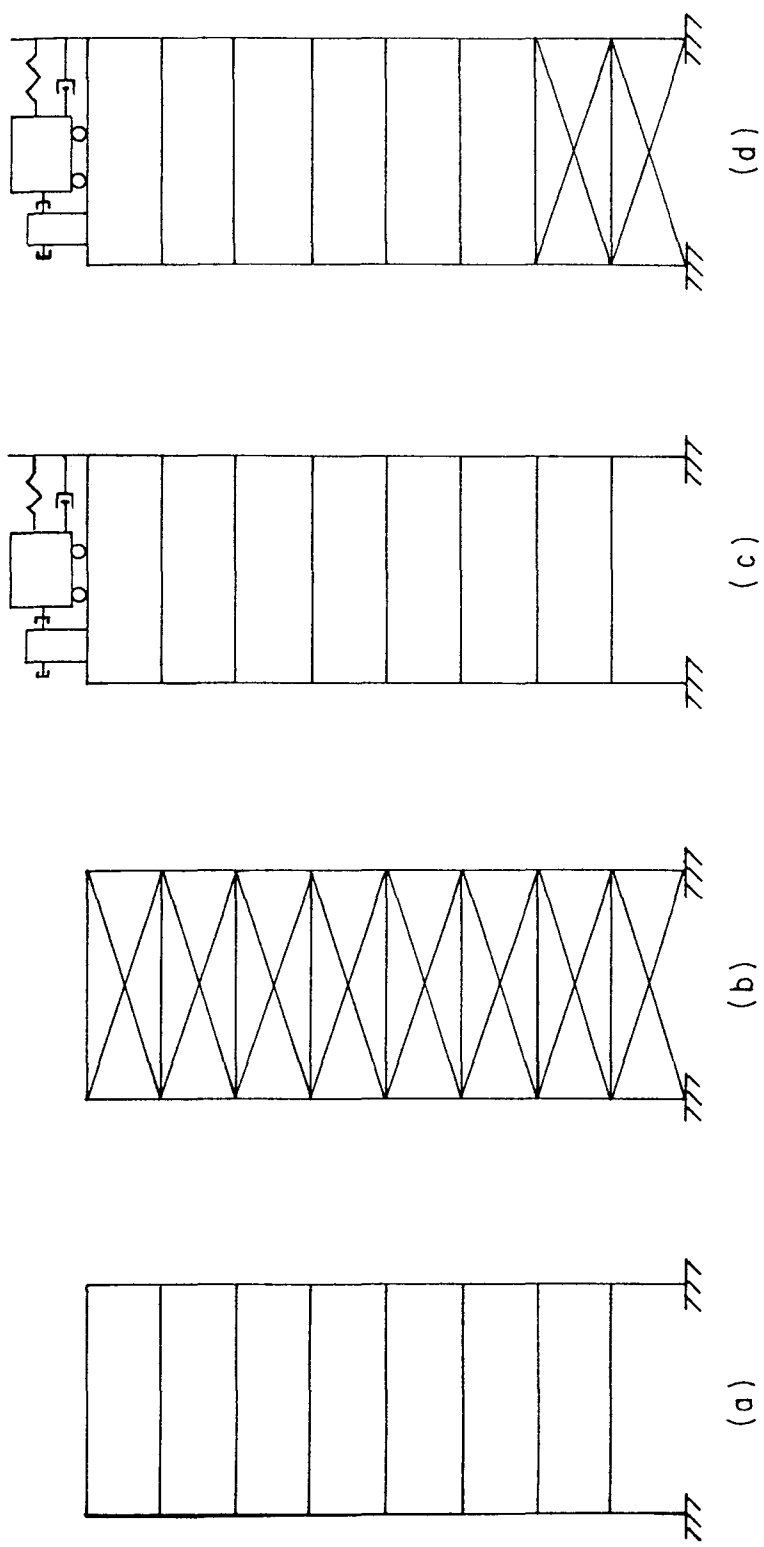
FIGURE 2-8 Eight-story Structure: (a) Case 1, (b) Case 2, (c) Case 3, (d) Case 4
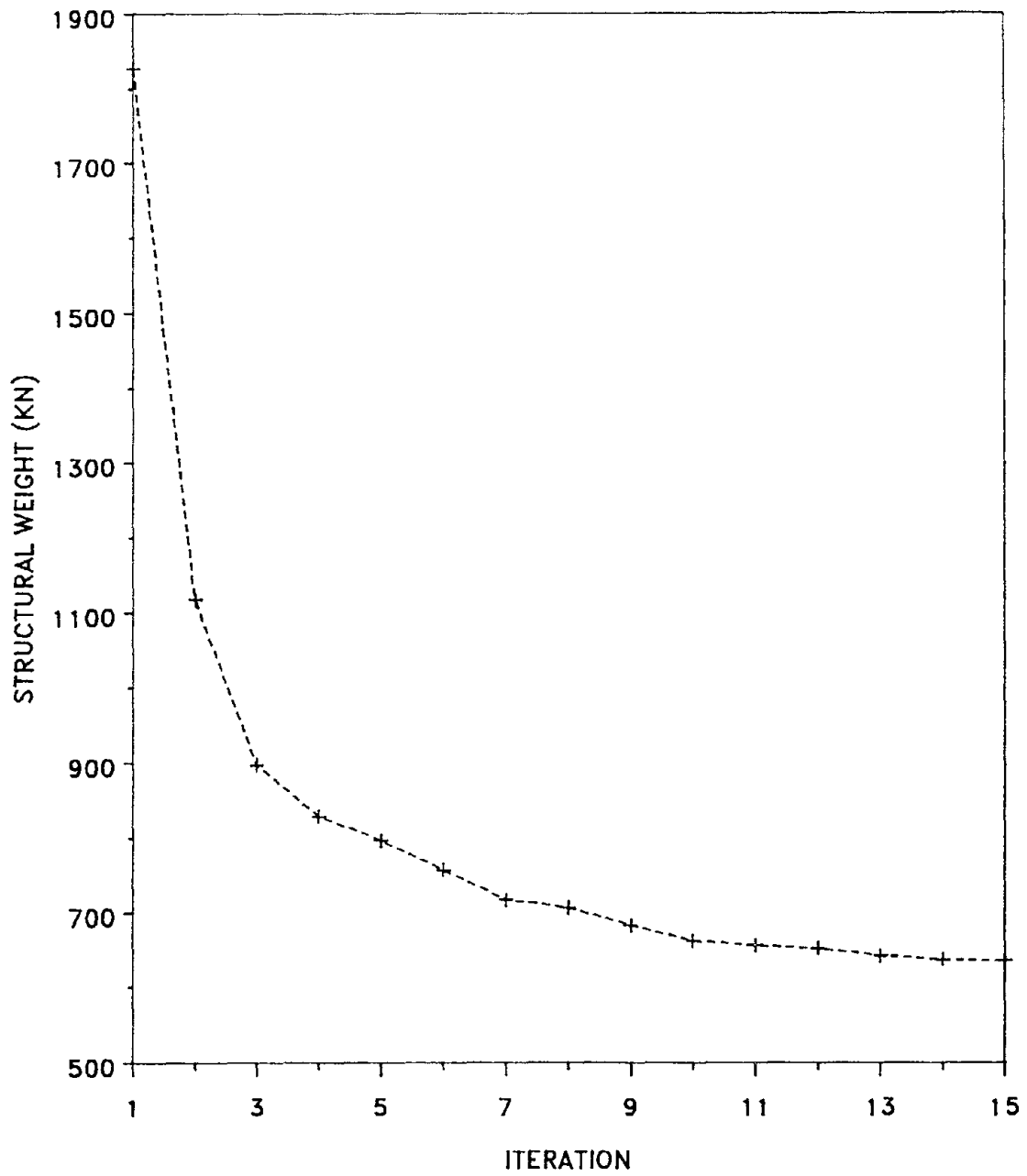
FIGURE 2-10 Structural Weight: Case 2 - Eight Active Tendons
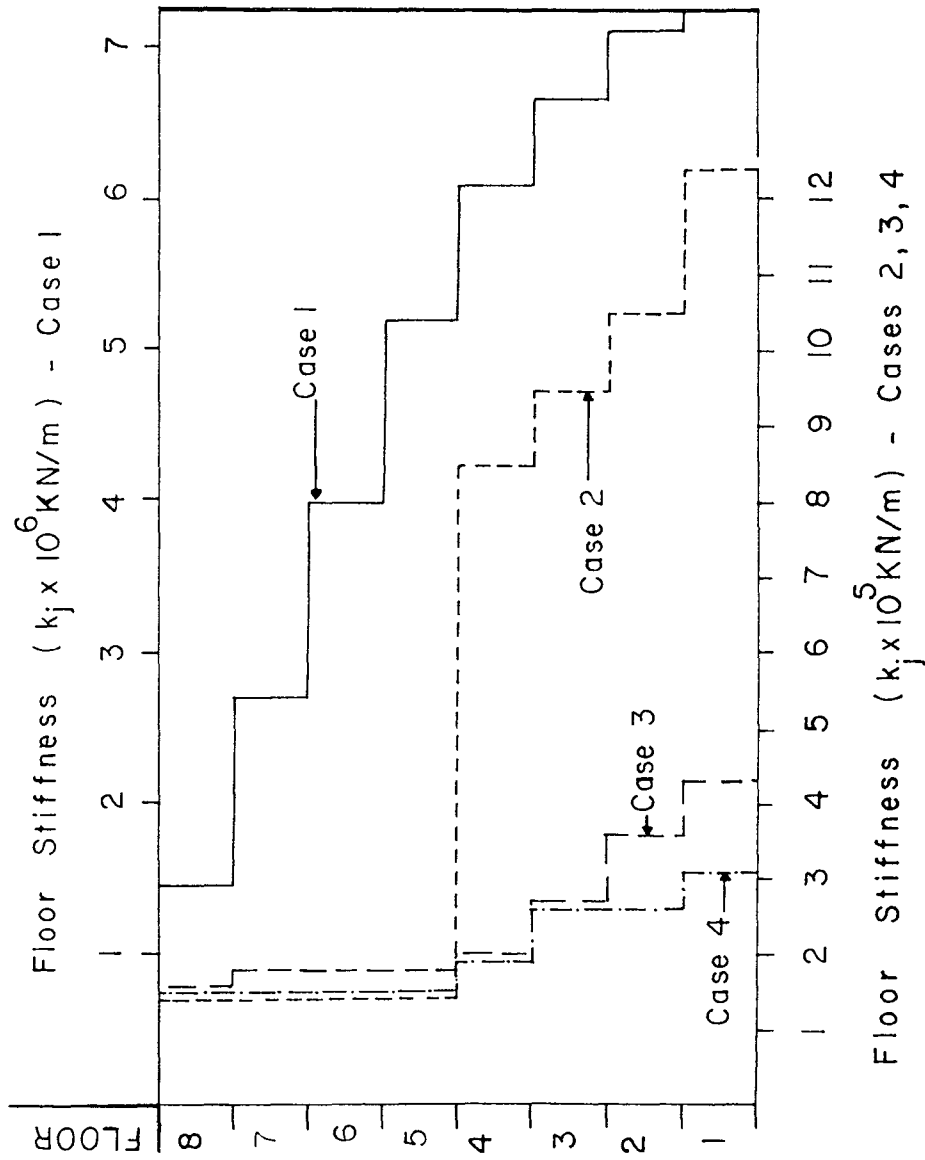
FIGURE 2-12 Optimum Stiffness Distribution: Cases 1-4
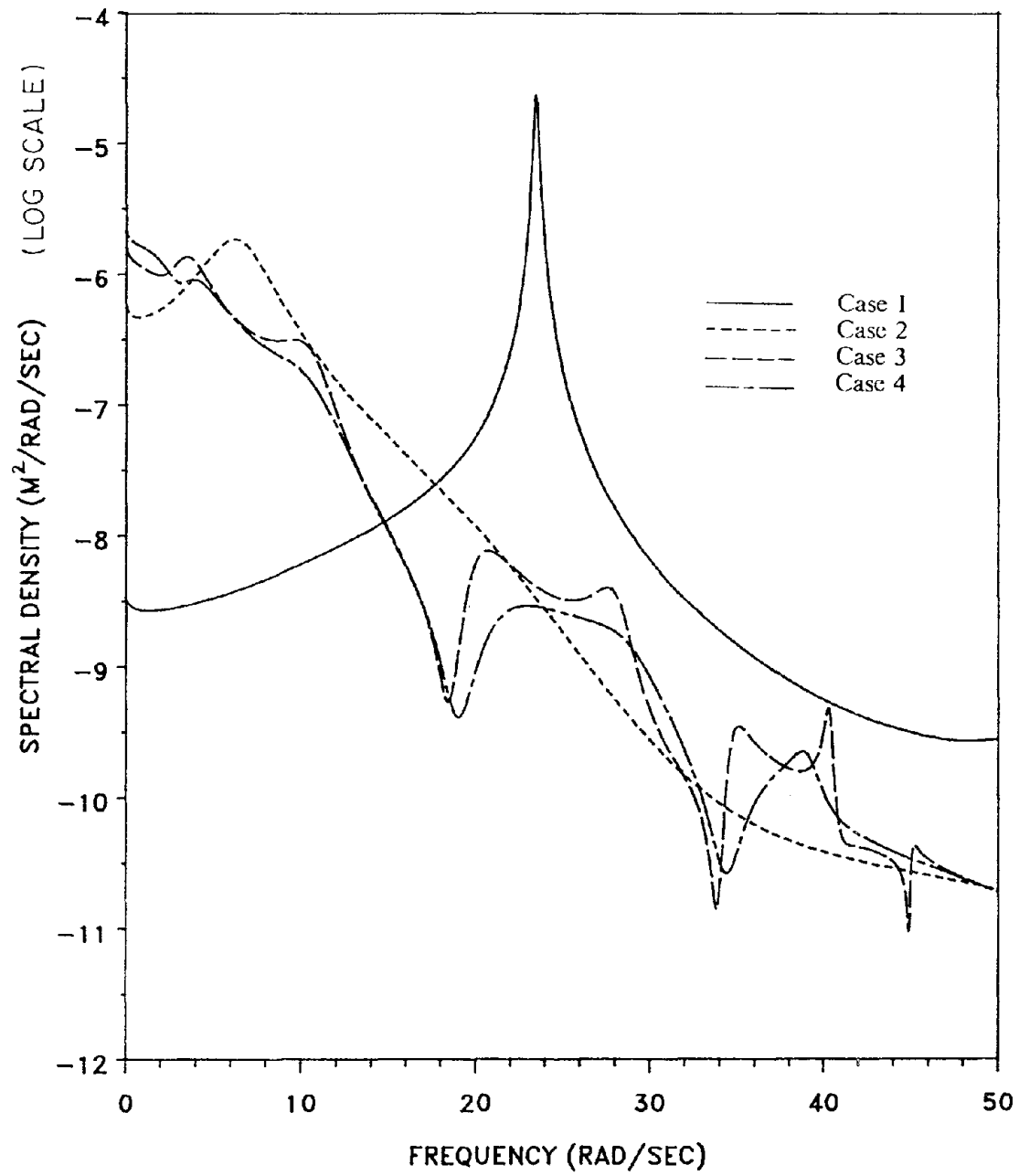
FIGURE 2-14   Spectral Density of Eighth Floor Relative Displacement
                for Cases 1-4

Thus the optimal control forces are computed from the measured base acceleration $\ddot{X}_g(t)$ and previous information at $(t-\Delta t)$, keeping the real-time on-line computational effort minimal.

Instantaneous Closed-Loop

The control forces are regulated by the feedback response state-vector $\{z(t)\}$ alone, i.e. the only measurements required are those of the response at time t. There is a definite advantage of this algorithm for the case of wind excitation which is difficult to measure for application with the open-loop algorithm. The optimal control in this case is derived as

$$\{u^*(t)\} = -\ (\frac{\Delta t}{2})[R]^{-1}[B]^T[Q]\{z(t)\} \tag{20}$$

Note that another advantage of the instantaneous closed-loop algorithm is that it is insensitive to estimation errors in the stiffness, mass or damping of the structure since $[R]$, $[B]$ and $[Q]$ are known.

Instantaneous Open-closed-loop

This algorithm requires the measurement of the ground excitation and the response. The optimal control $\{u^*(t)\}$ is to be of the form

$$\{u^*(t)\} = [S1]\{z(t)\} + \{S2(t)\} \tag{21}$$

where $[S1]$ is a constant gain matrix, and $\{S2(t)\}$ a vector containing the measured excitation upto and including time t.

It can be shown that $[S1]$ and $\{S2(t)\}$ are given by

$$[S1] = -(\frac{\Delta t}{4})[R]^{-1}[B]^T[[I] + [Q][B][R]^{-1}[B]^T \frac{(\Delta t)^2}{8}]^{-1}[Q] \tag{22}$$

$$\{S2(t)\} = [S1]\{[T]\{\Lambda(t-\Delta t)\} + \{C\}\ddot{X}_g(t)(\frac{\Delta t}{2})\} \tag{23}$$

The derivations for the active mass damper control system shown in Figure 3-1(b) are similar to those for the active tendon, and are not given here.

3-3

u_d max = allowable AMD control force

Based on a rational stiffness distribution, an optimum structure will be obtained in accordance with the allowable level of the control forces.

3.3 Control Energy Minimization

Numerical simulations show that when the elements of the response weighting matrix [Q] are large the response is reduced, but at the expense of large control forces.   When the elements of the control weighting matrix [R] are large the control forces are small, however the displacement response is not reduced appreciably.

Physical limitations of the actuator impose an upper bound on the maximum control force magnitude that can be achieved. Considerations of power limit the control energy available. Various objectives and constraints can be met by judicious selection of the elements of the weighting matrices. Physically the weighting matrices affect the gain matrix for the system and they are implemented in terms of the amplifier gains that produce the control forces.

A rational procedure is developed herein in order to obtain the optimal weighting matrix [R]. The elements of matrix [Q], and the structural stiffnesses are kept constant. The control energy is chosen as the objective function to be minimized. The constraints are the same as those used in the structural optimization. The optimization problem is as follows: Find the elements R(i,i) of the weighting matrix [R] assumed diagonal, that will minimize the control energy defined as

$$JE = \frac{1}{2} \int_0^{t_f} \{u(t)\}^T [R] \{u(t)\} \ dt \qquad (28)$$

subject to constraints on the allowable floor relative displacements and allowable control forces of Eqs. (24-27). The objective here is to obtain the optimum weighting matrices that will reduce the control forces, while the response still remains within the constraint limitations.   In this

3-5

no-control case, it is evident that for the rest of the time history, the reduction is much greater. The maximum relative velocity and maximum acceleration of the eighth floor have been respectively reduced by 55% and 70% as compared to the no-control case.

From Figure 3-5, the eighth floor relative displacement has been reduced by using the active mass damper system by about 80% as compared to the no-control case. The maximum relative velocity and acceleration of the eighth floor have both been reduced by 85% as compared to the no-control cases. The damper control force is about one third of the allowable at its maximum value. This is the reason why the active mass damper system does not reduce the response as much as the active tendon system. However, the active mass damper performance could be improved by adjusting the elements of the weighting matrices, so as to yield a large control force.

3.4.2 Example 4: Optimum Structure Using Closed-Loop Control

The instantaneous optimal closed-loop control algorithm is used in this example to illustrate the benefits of combining structural optimization with active control. An eight-story shear building is considered. The structural properties are: m_j = 2 kip - sec^2/in (350 Mg), j = 1,...,8, and 1% critical damping in all the modes. The earthquake excitation used is the N-S component of the El-Centro earthquake of May 18, 1940. The structure is equipped with eight active tendons, one on each floor. The weighting matrices [Q] and [R], are assumed diagonal with the values R(i,i) = 0.06, i = 1,...,8 and Q(l,l) = 1500, l = 1,...,16. The choice of these matrices at this stage is arbitrary, and they are fixed at this values during the structural optimization.

The constraints used in this case (Case 1) are: x_1 max = 0.72 in (.018 m), x_2 max = 1.44 in (.037 m), x_3 max = 2.16 in (0.55 m), x_4 max = 2.88 in (.073 m), x_5 max = 3.60 in (.091 m), x_6 max = 4.32 in (.110 m), x_7 max = 5.04 in (.128 m), x_8 max = 5.76 in (.146 m), u_i max = 300 kips (133 kN), i = 1,...,8, and k min = 400 kips/in (70040 kN/m). The optimization cycles for the structural weight are shown in Figure 3-6. The optimum stiffness distribution at the final interation is shown in Figure 3-7. The optimum
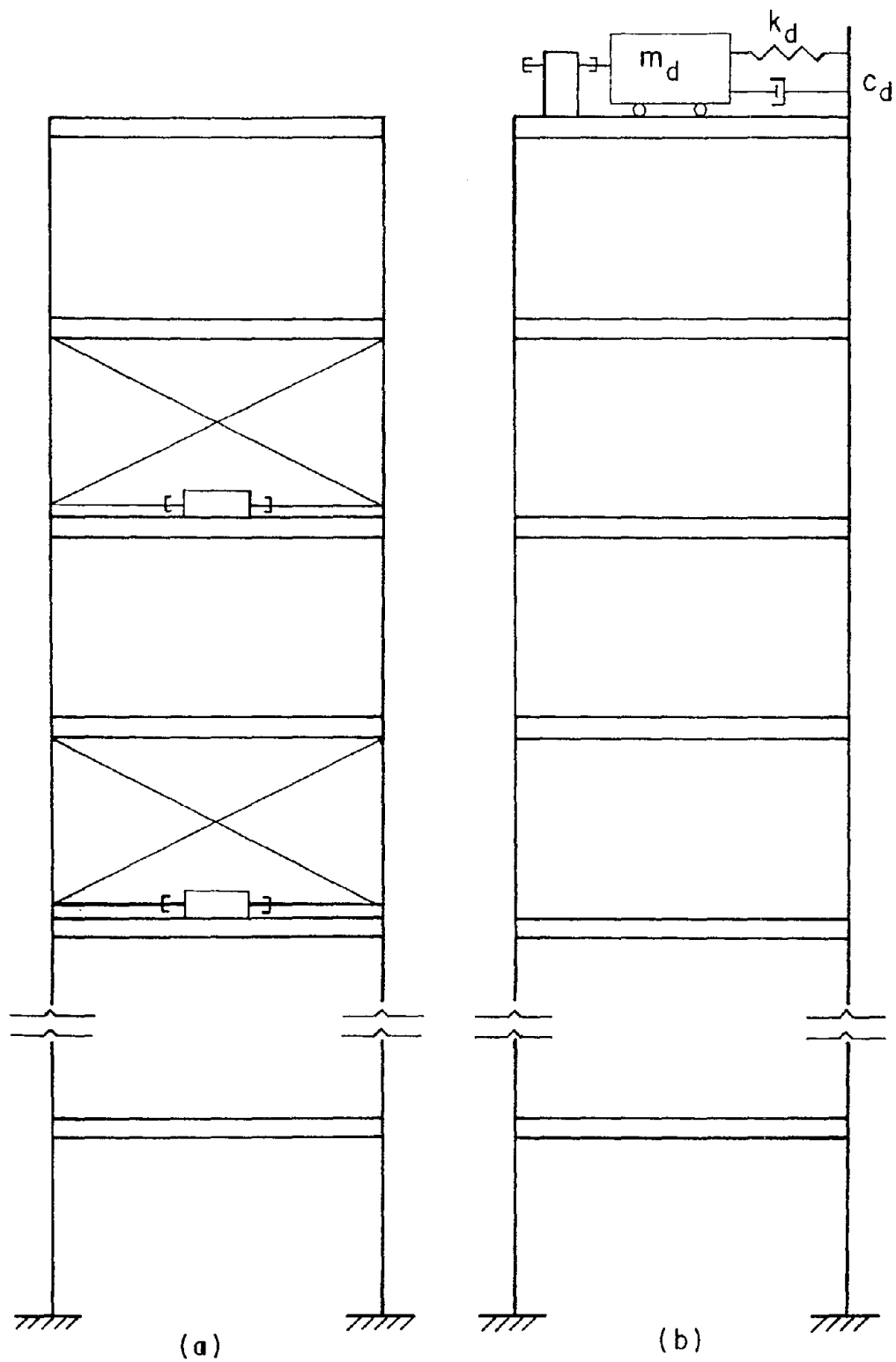
FIGURE 3-1   Tall Building Equipped with Active Control System:
(a) Active Tendon, (b) Active Mass Damper
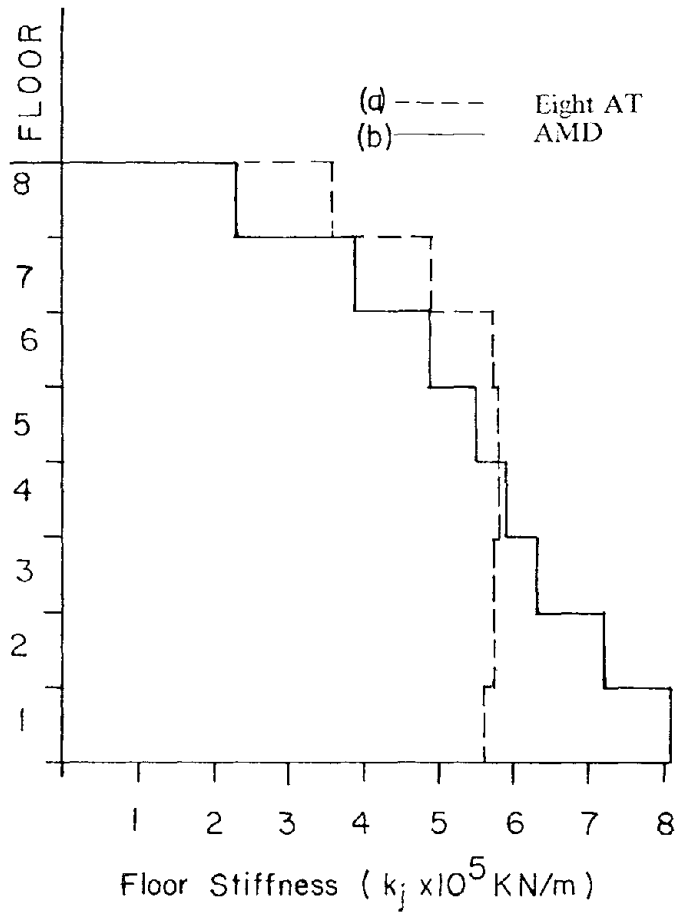
FIGURE 3-3 Optimum Stiffness Distribution for Building with:
(a) Eight Active Tendons, (b) Active Mass Damper
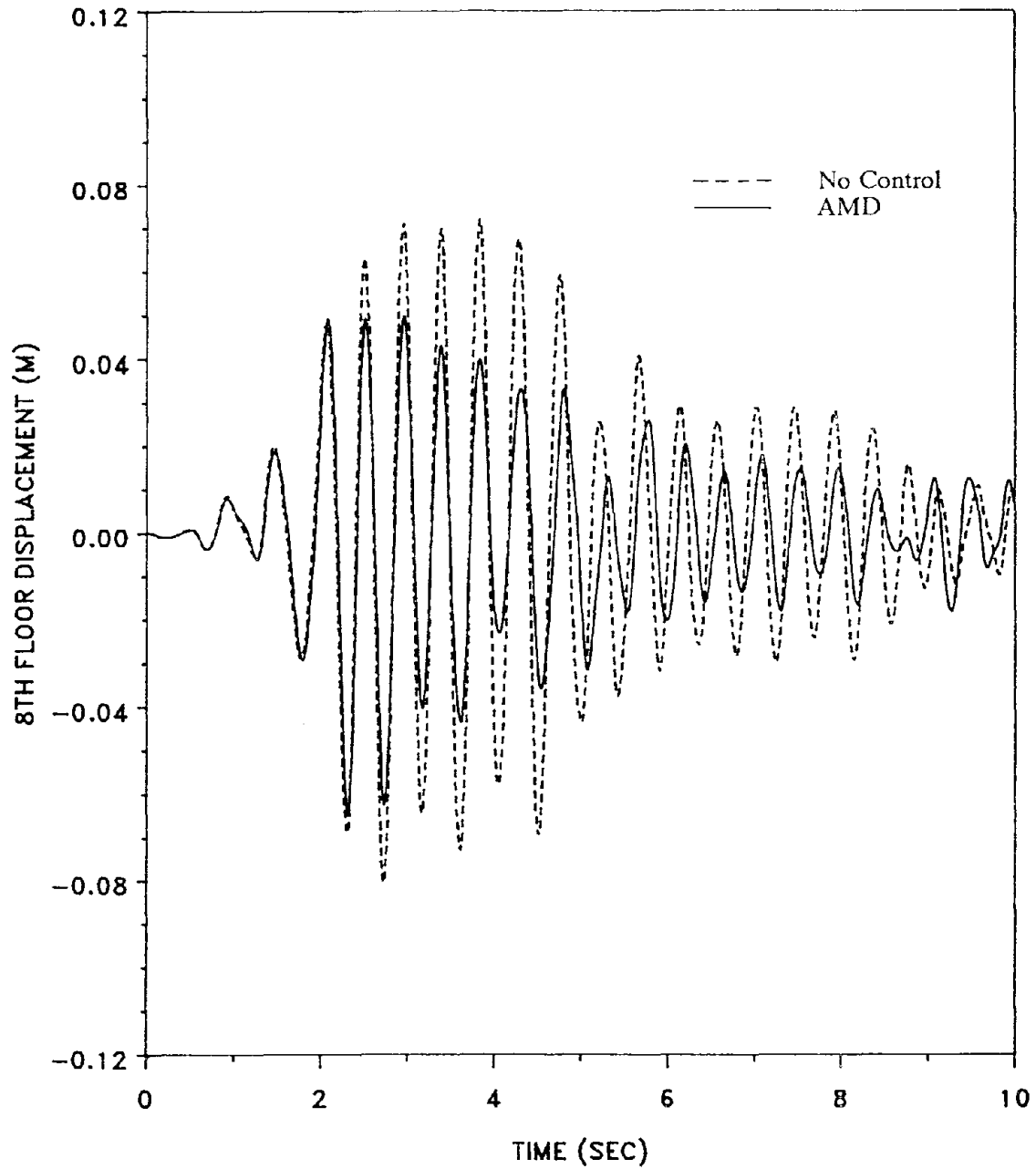
FIGURE 3-5   Comparison of Eighth Floor Relative Displacement of
Optimum Structure with and without Active Mass Damper
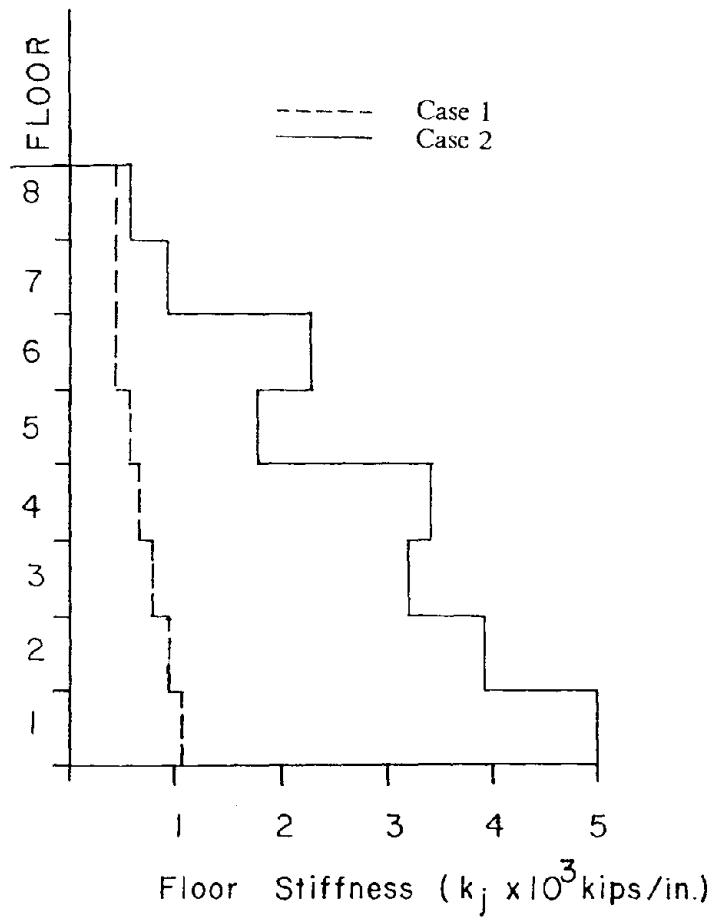
FIGURE 3-7 Optimum Stiffness Distribution for Cases 1 and 2

TABLE 3-I   CONTROL ENERGY MINIMIZATION RESULTS

Maxima of Control Forces (kip)
(1 kip = 4.45 kN)

Iteration Number	Floor Number							
	1	2	3	4	5	6	7	8
1	289	271	285	280	273	252	177	92
5	250	258	211	216	202	162	89	57

Weighting Variables $R(i,i) \times 10^{-3}$

Iteration Number	Floor Number							
	1	2	3	4	5	6	7	8
1	.070	.070	.070	.070	.070	.070	.070	.070
5	.110	.076	.100	.095	.109	.169	.274	.240

SECTION 4

CRITICAL-MODE CONTROL

The optimal critical-mode control algorithm is likely to be as effective as the optimal global control, since the response of tall buildings under earthquake excitations is usually dominated by a few lowest modes. The critical-mode control is also superior to the global control, as far as the amount of on-line computations is concerned. For global control of a structure with N degrees of freedom, the instantaneous closed-loop algorithm requires the solution of 2N differential equations. However if only $\overline{m}$ critical modes are controlled where ($\overline{m}$<N), only $2\overline{m}$ differential equations have to be solved. The critical-mode control algorithm is developed herein in order to reduce the amount of computation, and is also used to study the optimal locations of controllers.

4.1 Critical-Mode Control Formulation

The formulation is developed using the instantaneous closed-loop algorithm of Section 3.1 for the active tendon system. The state-equation, Eq. (15), can be transformed into the modal domain as follows

$$\{z(t)\} = [T]\{\psi(t)\} \tag{29}$$

in which [T] is given by

$$[T] = [\{M_1\}, \{Y_1\}, \ldots, , \{M_j\}, \{Y_j\}, \ldots, \{M_N\}, \{Y_N\}] \tag{30}$$

where:

$\{M_j\}$ = real part of jth eigenvector

$\{Y_j\}$ = imaginary part of jth eigenvector

Substituting Eq. (29) in Eq. (15) yields

$$[T]\{\dot{\psi}(t)\} = [A][T]\{\psi(t)\} + [B]\{u(t)\} + \{C\}\ddot{X}_g(t) \tag{31}$$

Premultiplying Eq. (31) by $[T]^{-1}$ yields the modal state-equation

4-1

Substituting the partitioned modal state-vector $\{\psi(t)\}$

$$\{\psi(t)\} = \left\{ \frac{\{\psi(t)_c\}}{\{\psi(t)_r\}} \right\} \tag{37}$$

in Eq. (36), and ignoring terms that involve the residual modes the critical-mode performance index is

$$J_c(t) = \{\psi(t)\}_c^T [Q]_c \{\psi(t)\}_c + \{u(t)\}^T [R]\{u(t)\} \tag{38}$$

in which $[Q]_c$ is a $\overline{2m}$ x $\overline{2m}$ matrix obtained form partitioning the following matrix product

$$[T]^T[Q][T] = \left[\begin{array}{c|c} [Q]_c & [Q]_{cr} \\ \hline [Q]_{rc} & [Q]_r \end{array} \right] \tag{39}$$

The critical-mode optimal control problem is stated as: Find the optimal control $\{u^*(t)\}$, that minimizes the critical-mode performance index $J_c(t)$ of Eq. (38) and satisfies the state-equation for the critical modes, Eq. (34). The critical-mode closed-loop optimal control is found [ref. 16], as

$$\{u^*(t)\} = -[\frac{\Delta t}{2}][R]^{-1}[TB]_c^T [Q]_c \{\psi(t)\}_c = [K]_c \{\psi(t)\}_c \tag{40}$$

Note that the optimal control is given as a function of the modal state-vector. Specifically, only the critical modes $\{\psi(t)\}_c$ are of interest. However the displacement and velocity sensors measure the actual state-vector $\{z(t)\}$. The modal states can be estimated using modal filters, as pointed out by Meirovitch and Baruh $\left[\text{ref. } 22 \, . \right]$ The modal filters produce estimates of modal states from distributed measurements of the actual states. For simulation purposes we assume here that the modal state-vector can be recovered from the actual state-vector $\{z(t)\}$ by using the inverse of Eq. (29) in the form

$$\left\{ \frac{\{\psi(t)\}_c}{\{\psi(t)\}_r} \right\} = [T]^{-1}\{z(t)\} \tag{41}$$

A comparison of the global instantaneous closed-loop algorithm and the critical-mode control algorithm is carried out. An eight-story shear building is considered whose structural properties of stiffness, mass and damping are: k_1 = 1026.3 kip/in (179700 kN/m), k_2 = 937.4 kip/in (164140 kN/m), k_3 = 790.6 kip/in (138430 kN/m), k_4 = 684.1 kip/in (119790 kN/m), k_5 = 538.5 kip/in (94290 kN/m), k_6 = 400.0 kip/in (70040 kN/m), k_7 = 400.0 kip/in (70040 kN/m), k_8 = 400.0 kip/in (70040 kN/m), m_j = 2 kip-sec^2/in (350 Mg), j = 1,...,8, and 3% critical damping in all the modes. The earthquake excitation used is the N-S component of the El-Centro earthquake of May 18, 1940. The structure is equipped with eight active tendons, one on each floor. The weighting matrices [Q], and [R], are assumed diagonal with the values R(i,i) = 0.06, i = 1,...,8 and Q(l,l) = 1500, l = 1,...,16. The global algorithm considers control of all eight modes and the critical-mode algorithm considers control of only the first and second mode. Figure 4-1 shows the eighth floor relative displacement. It can be observed that the two-mode control is almost as effective as the global control for this structure and excitation. The two algorithms also require control forces of similar magnitude.

4.3.2 Example 7: Spillover Effect

The structure of Section 4.3.1 equipped with only two active tendons located at the two bottom floors is subjected to an artificial earthquake ground acceleration. The excitation is a combination of three sinusoids centered around the first, second and third frequencies of the structure of 3.5 rad/sec, 9 rad/sec and 15 rad/sec respectively. These sinusoids are weighted and scaled to reflect a peak magnitude of ground acceleration of 0.2 g and to excite the first three modes. The purpose here is to evaluate the spillover effect. The artificial excitation, designated as Excitation 1, is given by

$$\ddot{X}_g(t) = .05 \ g \ (.2 \sin 3.5 \ t + \sin 9 \ t + 3 \sin 15 \ t) \tag{45}$$

The critical mode algorithm was used to control the first and second mode. The eighth floor relative displacement is split into the modal contributions of the first three modes, and is compared with the no-control case. Figure

4-5
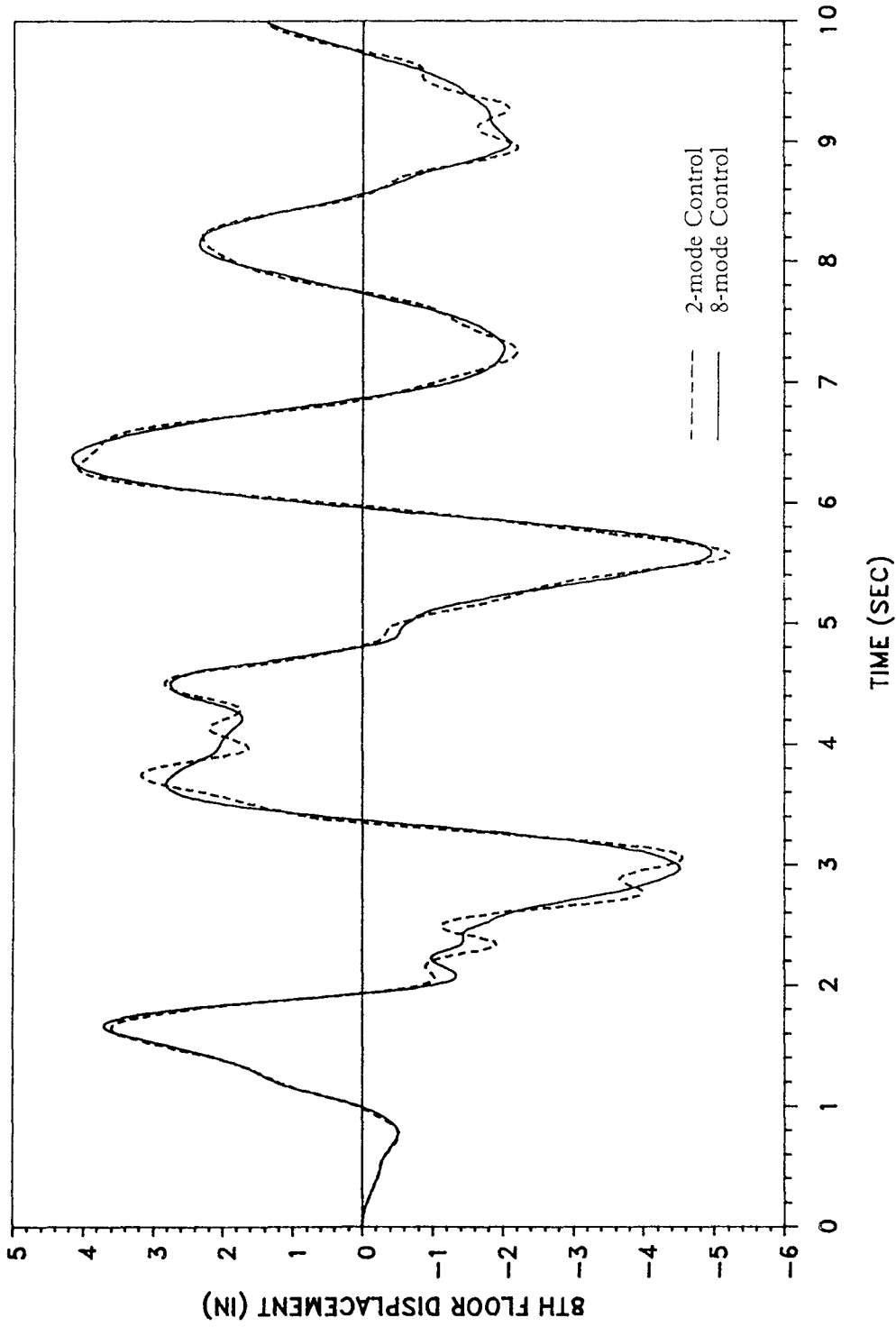
FIGURE 4-1 Response for Global and Critical-mode Control
(1 in = 25.4 mm)

4-7
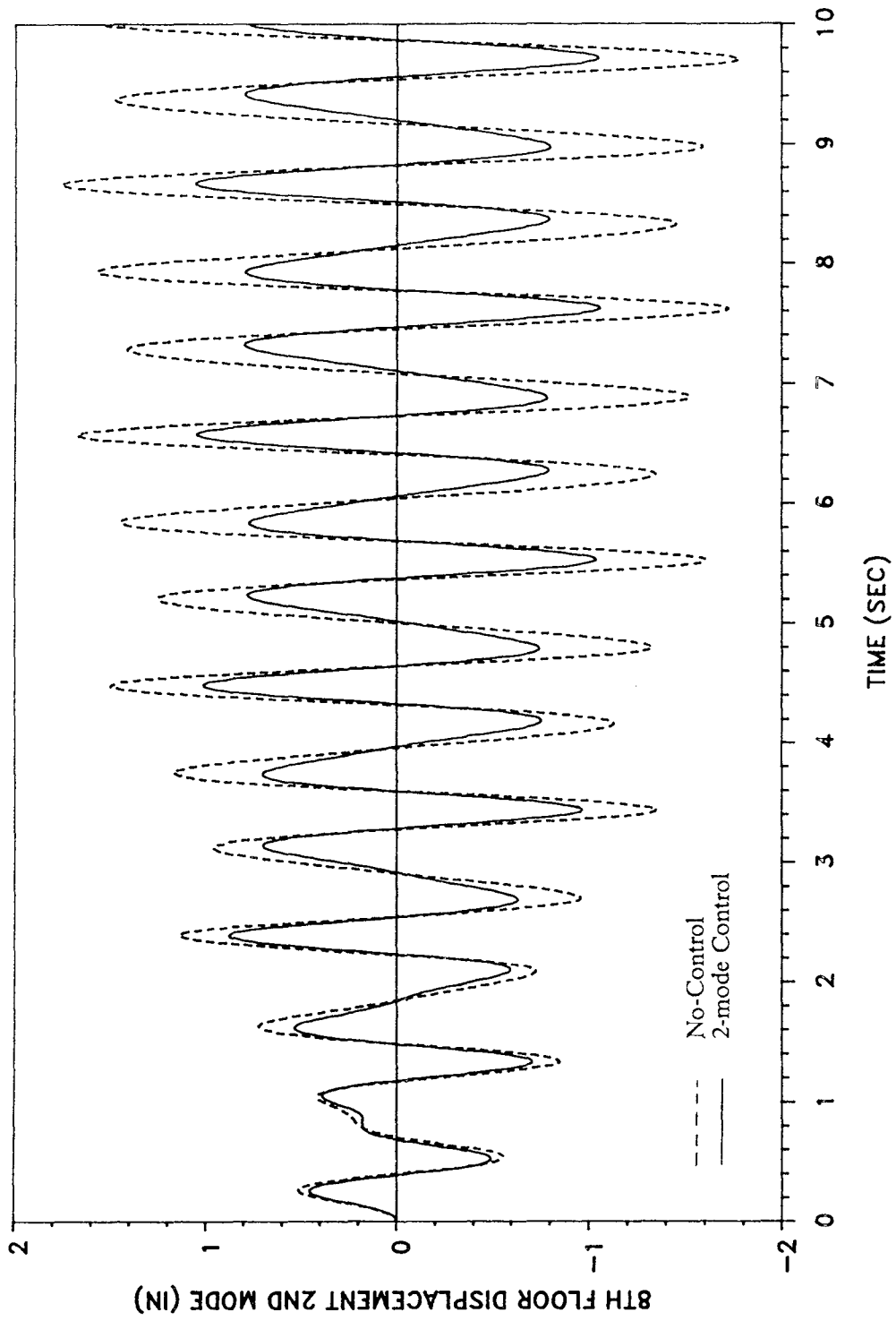
FIGURE 4-3 Second Mode Response for Critical-mode Control
(1 in = 25.4 mm)

SECTION 5

OPTIMAL LOCATION OF CONTROLLERS

The objective here is to establish criteria for the optimal location of a limited number of controllers. The critical-mode optimal control algorithm is used to control the lowest modes of a seismic structure. It is quite plausible that in the application of active control systems to structures, it may be more economical to place the controllers at a few preselected locations. The term optimal locations reflects on the reduction of the structural response, while using the minimum control effort. The location of the controllers with respect to the structure is reflected in the matrix $[\gamma]$ in Eq. (14), or the state-form matrix $[B]$ in Eq. (15). By varying the locations of the controllers, the entries in the aforementioned location matrix will be changed, thus the dynamic response will be modified.

5.1 Methods for Selecting Optimal Locations

One method of selecting the optimal controller locations is to consider the modal shapes of the structure. The modal shapes of the few lowest modes that we select to control give useful information about the most beneficial locations. The maxima of these modal shapes in a given mode are obviously advantageous locations for the controllers. However the determination of the optimal locations for a combination of modes is more of an intuitive procedure, but nevertheless useful. Another method for the optimal locations selection is one proposed by Martin and Soong [ref. 20]. In this approach a performance index of control energy is minimized in the time period of interest. This performance index is defined by the integral

$$J_E = \int_0^{t_f} \{u(t)\}^T \{u(t)\} dt \tag{46}$$

where:

t_f = final time

The concept here is that if the choice of the controller locations is to be optimal, the control work performed by the control system as reflected in

5-1

for the 5th and 6th floor choice. The maxima of the control forces for the 5th and 6th floor choice is slightly greater.

For the same structure, another comparison is made between the two cases of modal shape and performance index choices. This time the elements of the weighting matrix [R] are allowed to be different in the two choices. The elements of matrix [Q] are still fixed. The reason for allowing the elements of matrix [R] to be different in the two choices is to make the maxima of the control forces for both choices equal. In this sense a better comparison can be carried out. The results of this comparison are shown in Table 5-II and Figures 5-2 through 5-4. Both the control energy and response performance indices are less for the 5th and 6th floor choice. Similarly the maxima of the relative displacements and accelerations for all the floors are less for the 5th and 6th floor choice. The maxima of the control forces are equal and the elements of matrix [R] are different as shown in Table 5-II. A comparison of the required control forces for the two choices indicates that they are approximately equal. The 5th and 6th floor choice reduces the 8th floor response more effectively as can be seen from Figures 5-2 and 5-3 for the first and second mode response. From Figure 5-4 we can observe the spillover effect on both choices.

A second artificial excitation, Excitation 2, is applied to the same structure. Excitation 2 is given as

$$\ddot{X}_g(t) = .02 \ g \ (.2 \ \sin 3.5 \ t + 7. \ \sin 9 \ t + 3.3 \ \sin 15 \ t) \qquad (48)$$

It excites the second mode more than the other modes. As before, the elements of the weighting matrix [R] are different in the two choices. The elements of matrix [Q] are fixed. The results are shown in Table 5-II. The 5th and 6th floor choice is still better than the modal choice of 4th and 8th floor. Note that the response index is less and control energy is higher for the 5th and 6th floor choice. The simulation shows that the response response index may be a better measurement than the control energy. The two choices are compared, and overall the performance index choice of 5th and 6th floors is better. A note needs to be made about the modal choice. It is interesting to note that after a modal choice has been made,

TABLE 5-I OPTIMAL CONTROLLER LOCATIONS : FIXED R(I,I) - EXCITATION 1
(1 kip = 4.45 kN), (1 in = 25.4 mm)

Locations	4 & 8	5 & 6
Control Energy	74829	74132
Response Index	368	266
Maximum Displacement	(in.)	(in.)
Floor 1	1.94	1.72
Floor 2	3.27	2.95
Floor 3	3.43	3.21
Floor 4	3.40	2.45
Floor 5	5.95	4.74
Floor 6	6.67	5.78
Floor 7	5.61	4.16
Floor 8	8.64	6.89
Maximum Acceleration	(% g)	(% g)
Floor 1	90	80
Floor 2	146	127
Floor 3	134	109
Floor 4	55	40
Floor 5	148	140
Floor 6	189	173
Floor 7	59	47
Floor 8	179	152
	(kip)	(kip)
Maximum	4th 8th	5th 6th
Control Forces	92 164	95 179
R(1,1)	.15	.15
R(2,2)	.15	.15

TABLE 5-III OPTIMAL CONTROLLER LOCATIONS - EXCITATION 2
(1 kip = 4.45 kN), (1 in = 25.4 mm)

| Locations	4 & 8	5 & 6
Control Energy	124996	130195
Response Index	604	480
Maximum Displacement	(in.)	(in.)
Floor 1	2.77	2.39
Floor 2	5.07	4.37
Floor 3	6.39	5.46
Floor 4	6.39	5.39
Floor 5	6.05	5.25
Floor 6	3.65	4.05
Floor 7	6.49	6.05
Floor 8	8.75	8.18
Maximum Acceleration	(% g)	(% g)
Floor 1	298	80
Floor 2	149	127
Floor 3	138	110
Floor 4	55	41
Floor 5	149	138
Floor 6	189	172
Floor 7	57	47
Floor 8	180	152
	(kip)	(kip)
Maximum	4th 8th	5th 6th
Control Forces	150 152	153 152
$R(1,1)$	.075	.30
$R(2,2)$	.620	.720
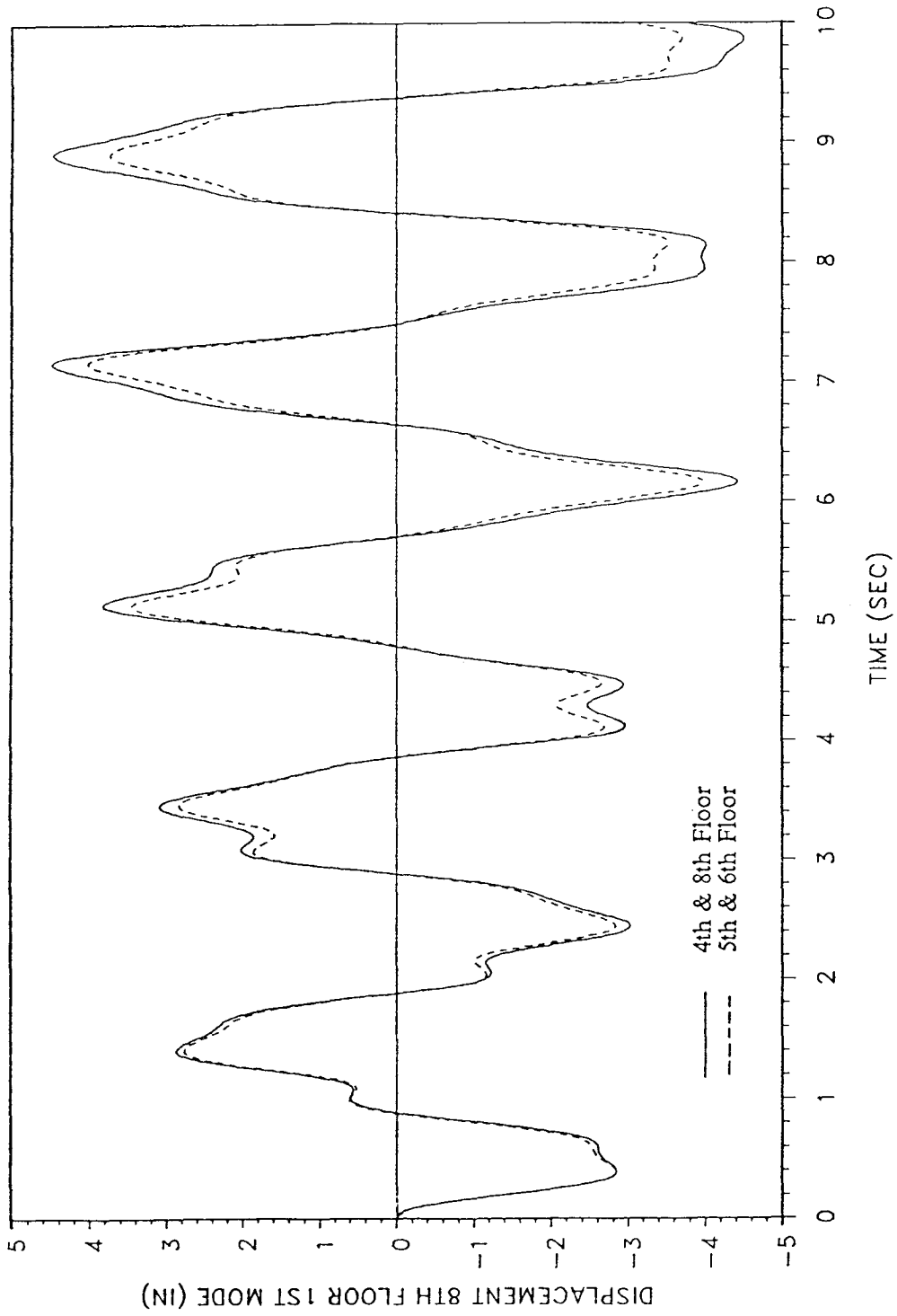
FIGURE 5-2 Controller Choices: First Mode Response - Excitation 1
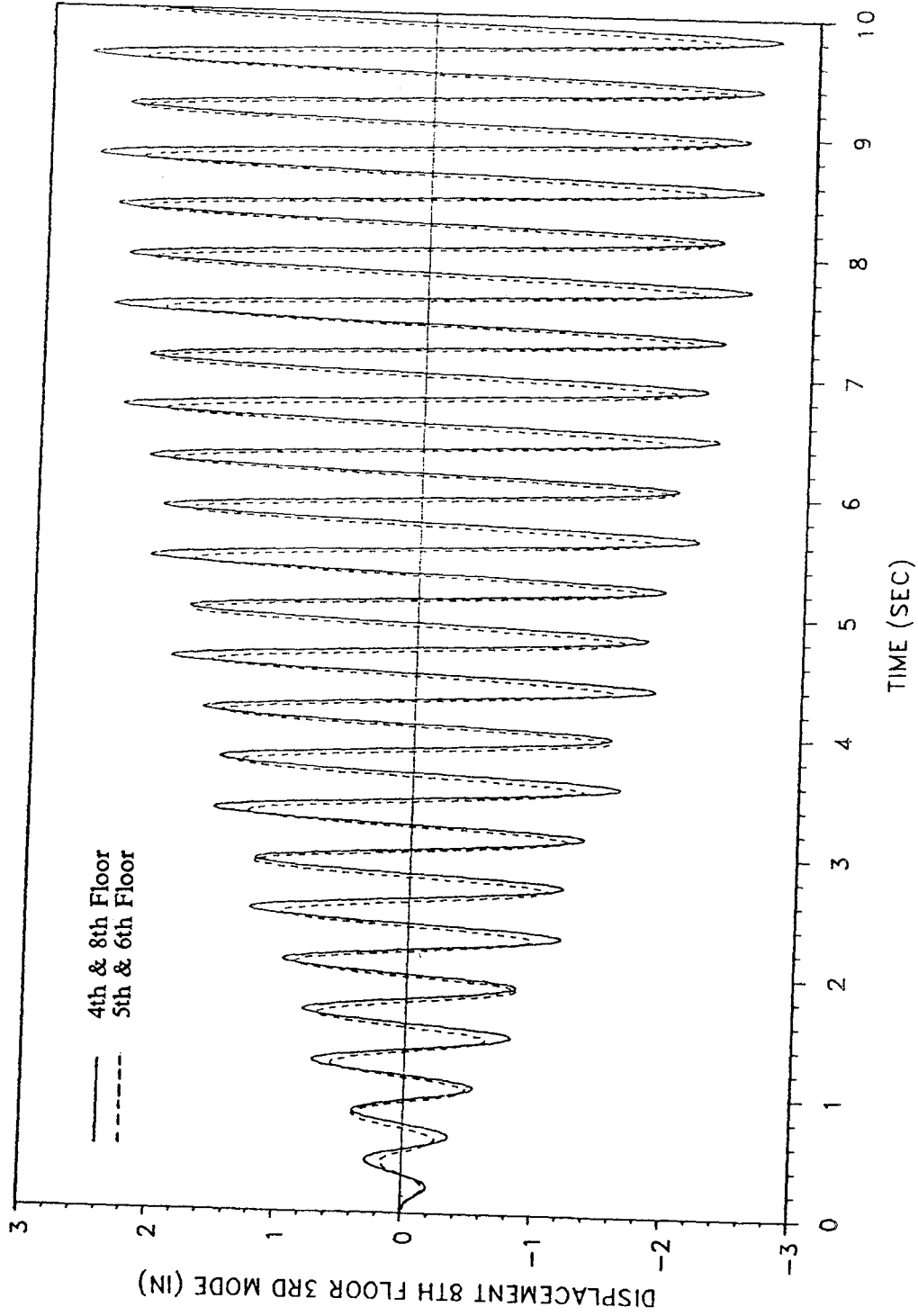(1 in = 25.4 mm)

5-9

FIGURE 5-4 Controller Choices: Third Mode Response - Excitation 1
(1 in = 25.4 mm)

SECTION 6

CONCLUSIONS

Active control of seismic structures can enhance their capacity to resist earthquake excitations over a wide range of exciting frequencies. Structural optimization is a rational and reliable design concept. A combining of structural optimization and structural control can yield an economical, and serviceable structure and its control forces.

The non-optimal closed-loop algorithm has the advantage that no on-line calculations are required for its implementation. For seismic structures it was found that the combination of the active mass damper and a number of active tendons is the most effective system since the active mass damper has the ability to reduce the first mode response and the active tendons control the higher modes.

An advantage of the instantaneous closed-loop algorithm as compared to the instantaneous open-loop and open-closed-loop, is that it is insensitive to estimation errors in the stiffness, mass or damping of the structure. This is because the gain matrix of the optimal control forces does not involve any of the structural properties.

A critical-mode optimal closed-loop algorithm was developed, based on the instantaneous closed-loop algorithm. The spillover effect was shown to be considerable. For seismic structures the prospect of applying the critical-mode control is very promising since the response is governed by the lowest few modes.

Three approaches for determining the optimal locations of a limited number of controllers have been investigated. The first approach is based on the modal shapes of the uncontrolled structure. However these modal shapes are changed when the control system is enforced and therefore the optimal locations may be difficult to be determined. The second and third are based on finding the locations of controllers that will minimize the control energy index and response index, respectively. The later two approaches are preferable and this can be attributed to the more rational procedure of

SECTION 7

REFERENCES

1. Balas, M., "Modal Control of Certain Flexible Systems", SIAM Journal of Control and Optimization, Vol. 16, No. 3, May 1978, pp. 450-462.

2. Chang, J.C.H. and Soong, T.T., "Structural Control using Active Tuned Mass Dampers", J. Engrg. Mech. Div., ASCE, 106 (EM 12), 1980, pp. 1091-1098.

3. Cheng, F.Y. and Botkin, M.E., "Nonlinear Optimum Design of Dynamic Damped Frames", J. Struct. Div., Am. Soc. Civil Engrs., Vol. 102(ST3), March 1976, pp. 609-628.

4. Cheng, F.Y. and Juang, D.S., Optimum Design of Braced and Unbraced Frames Subjected to Static, Seismic, and Wind Forces with UBC, ATC-3 and TJ-11, National Science Foundation Report, 1985 (376 pages), NTIS PB87-162988/AS.

5. Cheng, F.Y. and Pantelides, C.P., "Optimal Control of Seismic Structures", Dynamic Response of Structures, G.C. Hart and R.B. Nelson, Eds., ASCE, New York, N.Y., 1986, pp. 764-771.

6. Cheng, F.Y. and Pantelides, C.P., "Optimization of Structures and Controls under Seismic Loading", Proceedings of International Conference on Computational Mechanics-86, Tokyo, 1986, Vol. II, pp. X-135 - X-140.

7. Cheng, F.Y. and Pantelides, C.P., "Optimum Seismic Structural Design with Tendon and Mass Damper Controls and Random Process", Recent Developments in Structural Optimization, F.Y. Cheng, Ed., ASCE, New York, N.Y. 1986, pp. 40-53.

8. Cheng, F.Y. and Pantelides, C.P. "Combining Structural Optimization and Active Control," Computer Applications in Structural Engineering, American Society of Civil Engineers, 1987, pp. 592-607.

9. Cheng, F.Y. and Pantelides C.P., "Optimal Active Control of Wind Structures Using Instantaneous Algorithm," Proceedings of the American Society of Mechanical Engineers, 1987, pp. 21-28.

10. Cheng, F.Y. and Juang, D.S., "Assessment of Various Code Provisions Based on Optimum Design of Steel Structures," International Journal of Earthquake Engineering and Structural Dynamics, 1988, Vol. 16, pp. 45-61.

11. Cheng, F.Y. and Chang, C.C., "Aseismic Structural Optimization with Safety Criteria and Code Provision," Proceedings of the U.S.-Asia Conference on Engineering for Mitigating Natural Hazards Damage, P. Karasudhi, P. Nutalaya, and A. Chiu, Eds., 1987, Vol. I, pp. D8-1-D8-12.

23. Meirovitch, L. and Oz, H., "Modal-Space Control of Large Flexible Spacecraft Possessing Ignorable Coordinates", Journal of Guidance and Control, Vol. 3, No. 6, Nov.-Dec. 1980, pp. 569-577.

24. Meirovitch, L. and Silverberg, L.M., "Control of Structures Subjected to Seismic Excitation", J. Engrg. Mech. Div., ASCE, Vol. 109, No. 2, April 1983, pp. 604-618.

25. Pantelides, C.P. "Optimal Design of Seismic and Wind Structures with Active Controls", Ph.D. Dissertation, Civil Engineering Department, University of Missouri-Rolla, 1987.

26. Prager, W. and Taylor, J.E., "Problems of Optimum Structural Design," J. Appl. Mech., Trans. Am. Soc. Mech. Engrs., 1968, Vol. 90, pp 102-106.

27. Prucz, A., Soong, T.T. and Reinhorn A., "An Analysis of Pulse Control for Simple Mechanical Systems", J. Dyn. Syst. Meas. Control, ASME, 107, 1985, pp. 123-131.

28. Soong, T.T. and Manolis, G.D., "Active Structures", J. Struct. Engrg., ASCE, Vol. 113, No. 11, Nov. 1987, pp. 2290-2302.

29. Soong, T.T. and Skinner, G.K., "Experimental Study of Active Structural Control", J. of Engrg. Mech. Div., ASCE, 107 (EM6), 1981, pp. 1057-1067.

30. Venkayya, V.B. and Cheng, F.Y., "Resizing of Frames Subjected to Ground Motion," Proc. Intl. Symp. on Earthquake Structural Engineering, F.Y. Cheng, Ed., 1976, Vol. I, pp. 597-612.

31. Venkayya, V.B., "Structural Optimization: A Review and Some Recommendations," Intl. J. Num. Methods Eng., 1978, Vol. 13, pp. 203-228.

32. Yang, J.N., "Control of Tall Buildings under Earthquake Excitation", J. Engrg. Mech. Div., ASCE 108 (EM5), 1982, pp. 833-849.

33. Yang, J.N., Akbarpour, A. and Gaemmaghami, P., "Instantaneous Optimal Control Laws for Tall Buildings Under Seismic Excitations", Technical Report NCEER-87-0007, June 10, 1987.

34. Yang, J.N. and Giannopoulos F., "Active Tendon Control of Structures", J. Engrg. Mech. Div., ASCE, 104 (EM3), pp. 551-568, 1978.

35. Yang, J.N. and Lin, M.J., "Optimal Critical-Mode Control of Building under Seismic Load", J. Engrg. Mech. Div., ASCE, Vol. 108, No. EM6, 1982, pp. 1167-1185.

36. Yang, J.N. and Lin, M.J., "Building Critical-Mode Control: Nonstationary Earthquake", J. Engrg. Mech. Div., ASCE, Vol. 109, No. EM6, 1983, pp. 1375-1389.

NATIONAL CENTER FOR EARTHQUAKE ENGINEERING RESEARCH
LIST OF PUBLISHED TECHNICAL REPORTS

The National Center for Earthquake Engineering Research (NCEER) publishes technical reports on a variety of subjects related to earthquake engineering written by authors funded through NCEER. These reports are available from both NCEER's Publications Department and the National Technical Information Service (NTIS). Requests for reports should be directed to the Publications Department, National Center for Earthquake Engineering Research, State University of New York at Buffalo, Red Jacket Quadrangle, Buffalo, New York 14261. Reports can also be requested through NTIS, 5285 Port Royal Road, Springfield, Virginia 22161. NTIS accession numbers are shown in parenthesis, if available.

NCEER-87-0001   "First-Year Program in Research, Education and Technology Transfer," 3/5/87, (PB88-134275/AS).

NCEER-87-0002   "Experimental Evaluation of Instantaneous Optimal Algorithms for Structural Control," by R.C. Lin, T.T. Soong and A.M. Reinhorn, 4/20/87, (PB88-134341/AS).

NCEER-87-0003   "Experimentation Using the Earthquake Simulation Facilities at University at Buffalo," by A.M. Reinhorn and R.L. Ketter, to be published.

NCEER-87-0004   "The System Characteristics and Performance of a Shaking Table," by J.S. Hwang, K.C. Chang and G.C. Lee, 6/1/87, (PB88-134259/AS).

NCEER-87-0005   "A Finite Element Formulation for Nonlinear Viscoplastic Material Using a Q Model," by O. Gyebi and G. Dasgupta.

NCEER-87-0006   "SMP - Algebraic Codes for Two and Three Dimensional Finite Element Formulations," by X. Lee and G. Dasgupta, to be published.

NCEER-87-0007   "Instantaneous Optimal Control Laws for Tall Buildings Under Seismic Excitations," by J.N. Yang, A. Akbarpour and P. Ghaemmaghami, 6/10/87, (PB88-134333/AS).

NCEER-87-0008   "IDARC: Inelastic Damage Analysis of Reinforced Concrete-Frame Shear-Wall Structures," by Y.J. Park, A.M. Reinhorn and S.K. Kunnath, 7/20/87, (PB88-134325/AS).

NCEER-87-0009   "Liquefaction Potential for New York State: A Preliminary Report on Sites in Manhattan and Buffalo," by M. Budhu, V. Vijayakumar, R.F. Giese and L. Baumgras, 8/31/87, (PB88-163704/AS).

NCEER-87-0010   "Vertical and Torsional Vibration of Foundations in Inhomogeneous Media," by A.S. Veletsos and K.W. Dotson, 6/1/87, (PB88-134291/AS).

NCEER-87-0011   "Seismic Probabilistic Risk Assessment and Seismic Margin Studies for Nuclear Power Plants," by Howard H.M. Hwang, 6/15/87, (PB88-134267/AS).

NCEER-87-0012   "Parametric Studies of Frequency Response of Secondary Systems Under Ground-Acceleration Excitations," by Y. Yong and Y.K. Lin, 6/10/87, (PB88-134309/AS).

NCEER-87-0013   "Frequency Response of Secondary Systems Under Seismic Excitations," by J.A. HoLung, J. Cai and Y.K. Lin, 7/31/87, (PB88-134317/AS).

NCEER-87-0014   "Modelling Earthquake Ground Motions in Seismically Active Regions Using Parametric Time Series Methods," G.W. Ellis and A.S. Cakmak, 8/25/87, (PB88-134283/AS).

NCEER-87-0015   "Detection and Assessment of Seismic Structural Damage," by E. DiPasquale and A.S. Cakmak, 8/25/87, (PB88-163712/AS).

NCEER-87-0016   "Pipeline Experiment at Parkfield, California," by J. Isenberg and E. Richardson, 9/15/87, (PB88-163720/AS).

NCEER-87-0017   "Digital Simulations of Seismic Ground Motion," by M. Shinozuka, G. Deodatis and T. Harada, 8/31/87, (PB88-155197/AS).